An Empirical Indoor Path Loss Model for Ultra-Wideband Channels

Saeed S. Ghassemzadeh, Larry J. Greenstein, Aleksandar Kavčić, Thorvardur Sveinsson, and Vahid Tarokh

Abstract: **We present a statistical model for the path loss of ultra-wideband (UWB) channels in indoor environments. In contrast to our previously reported measurements, the data reported here are for a bandwidth of 6GHz rather than 1.25GHz; they encompass commercial buildings in addition to single-family homes (20 of each); and local spatial averaging is included. As before, the center frequency is 5.0GHz. Separate models are given for commercial and residential environments and, within each category, for line-of-sight (LOS) and non-line-of-sight (NLS) paths. All four models have the same mathematical structure, differing only in their numerical parameters. The two new models (LOS and NLS) for residences closely match those derived from the previous measurements, thus affirming the stability of our path loss modeling. We find, also, that the path loss statistics for the two categories of buildings are quite similar.**

Index Terms: **Path loss, signal propagation, UWB.**

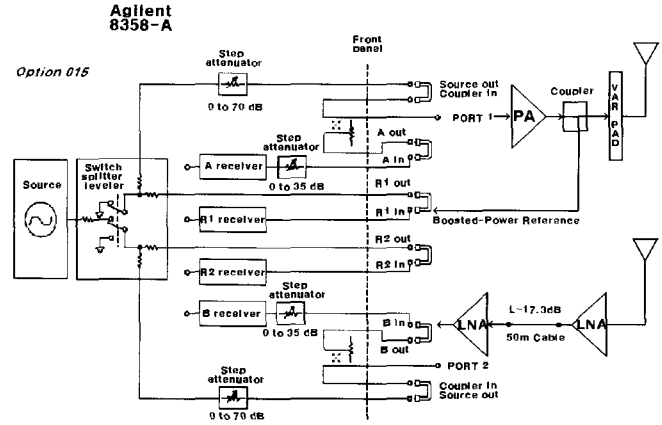

Fig. 1. Measurement transceiver configuration.

I. INTRODUCTION

Interest in commercial usage of ultra-wideband (UWB) communication systems has increased dramatically since the Federal Communication Commission (FCC) approved UWB transmission from 3.1–10.6GHz [1]. UWB technology is based on transmission of radar like signals, with its origin in military applications and short-range radar for locating and tracking. Following the approval of UWB for commercial usage, it is being considered as the physical layer for a new indoor wireless personal area networks (WPAN) standard [2]. The working environment of such networks would be indoor residential and commercial buildings. The propagation channel for UWB signals in such environments is the main focus of this paper.

Indoor signal propagation has been extensively studied over the past two decades, e.g., [3]–[6], although indoor measurements over very wide bandwidths are more recent, e.g., [7]–[12]. Here, we report on the large-scale propagation properties of a UWB channel in both residential and commercial indoor environments. Specifically, we construct a statistical model for the path loss in the environments of interest and conduct simulations confirming its goodness.

The organization of the paper is as follows: Section II covers the implementation of the measurements. Section III gives the basic path loss formula and describes the data reductions. Section IV presents the key findings. Finally, Section V gives the statistical path loss model and the results of our model simulations.

II. MEASUREMENT EQUIPMENT AND DATABASE

A. Equipment and Measurement Parameters

We use a vector network analyzer (e.g., PNA 8538A) to transmit 1601 continuous wave tones uniformly distributed from 2–8 GHz, with a frequency separation of 3.75MHz. This frequency resolution allows us to capture multipaths with maximum excess delay of 266ns. The 6GHz wide bandwidth gives a time resolution of 166.7ps.

The hardware setup of the experiment is as follows (see Fig. 1): The output port of the PNA is connected to a 30dB gain power amplifier (PA). The output power of the PA is returned to the reference port of the PNA to compensate for impedance mismatching between the PNA and PA. The boosted power is also connected to a variable attenuator followed by a conical monopole, 11GHz wide antenna with linear polarization. We use a conical monopole antenna radiating omni-directionally in the azimuth plane, with 0dBi gain in the range 1–12GHz. We were able to remove the antenna effects by calibrating the measurement equipment in an anechoic chamber.

A similar antenna receives the signal from the PNA and drives it through a low-noise amplifier (LNA) with a 34dB gain fol-

Manuscript received August 1, 2003.

S. S. Ghassemzadeh is with AT&T Labs-Research, Florham Park, NJ, USA, email: saeedg@research.att.com.

L. J. Greenstein is with WINLAB-Rutgers University, Piscataway, NJ, USA, email: ljg@winmain.rutgers.edu.

A. Kavčić, V. Tarokh, and T. Sveinsson are with Division of Engineering and Applied Sciences, Harvard University, Cambridge MA, USA, email: {kavcic, vahid}@deas.harvard.edu, vardi@kogun.is.

This material is based upon research supported in part by the National Science Foundation under grant no. CCR-0118701 and the Alan T. Waterman award, grant no. CCR-0139398. Any opinions, findings and conclusions or recommendation expressed in this publication are those of the authors and do not necessary reflect the views of the National Science Foundation.

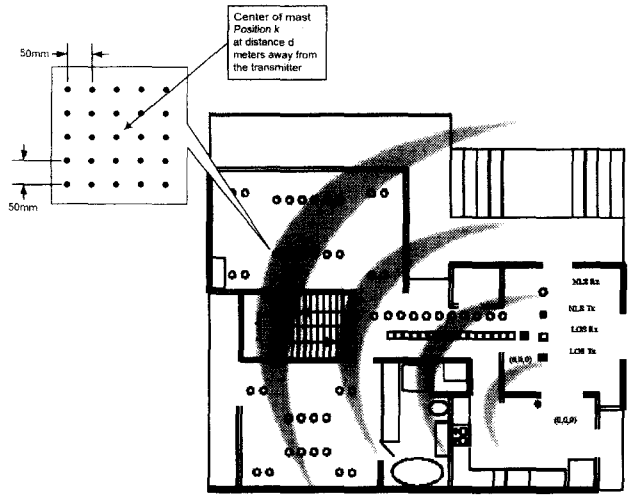

Fig. 2. Illustration of the spatial measurement set-up in a typical building.

lowed by a 45m long doubly-shielded ultra-low loss coax cable. The output of this cable is then amplified one last time by a 41dB gain LNA before it is received at the input of the same PNA for actual measurement. The measured complex frequency response is stored on a computer hard drive via a GPIB cable controlled by Agilent-VEE programs.

This set-up was properly calibrated in an anechoic chamber to compensate for the effects of impedance mismatching of the antennas with the front-end of the transceiver. The calibration data is also saved for post-processing and reduction of data.

B. Collected Database

The time-invariant nature of the indoor UWB channel has been shown in [10]. Hence, we measured only a single time-snapshot of the channel at each point in space. We captured the small-scale spatial variations of signal power by performing spatial measurements around each location, allowing us to construct the local spatial average of channel gain.

We measured 20 commercial buildings and 20 residences in the greater Boston area and in New Jersey. In each building, we selected around 30 locations, with transmitter-receiver (T-R) separation, d, ranging from 0.8m to 10.5m. We did this for both line-of-sight (LOS) and non-line-of-sight (NLS) paths. We refer to these points as local points. Around each local point, we performed 25 spatial measurements on a fixed grid. This is illustrated in Fig. 2. We refer to a single point on the grid as a spatial point. The distance between spatial points on the grid was 50mm. We performed all the measurements with transmitting and receiving antennas in the same horizontal plane; the height of the antennas was 1.8m.

III. PATH LOSS FORMULA AND DATA REDUCTIONS

A. Path Loss Formula

We define path loss as the dB reduction in power from the transmitter to the receiver location, where the received power is spatially averaged around the location. Specifically, it is averaged over an area whose radius is several wavelengths, with the wavelength being that at the center frequency of the transmission. A general path loss formula that incorporates reflection, diffraction and scattering for both LOS and NLS paths can be stated. It has the well-known form

$$PL(d) = PL_0 + 10\gamma \log_{10}(d/d_0) + S, \tag{1}$$

where PL_0 is the point at the reference distance d_0 and γ is the slope of the average increase in path loss with dB-distance. The spatial variation S denotes a zero-mean Gaussian random variable with standard deviation, σ. It can thus be written as $S = y\sigma$, where y is a zero-mean, unit-variance Gaussian random variable. The spatial variation of S is usually referred to as *shadowing*, and it captures the path loss deviation from its median value.

B. Data Reductions

After the removal of stored calibration data, for each local point, the database consists of 25 channel complex frequency responses, $H_k(f_i)$. Here, the index k denotes one of the 25 grid positions and the f_i are 1601 discrete frequencies ranging from 2-8 GHz (i.e., $1 \leq k \leq 25$ and $0 \leq i \leq 1600$). We define the *local path loss* (in dB) at grid position k and T-R separation d as

$$PL^k_{sp}(d) = -10\log_{10}\left(\frac{1}{1601}\sum_{i=0}^{1600}|H_k(d,f_i)|^2\right). \tag{2}$$

Note that the local path loss is relatively insensitive to frequency and therefore we represent it as an average over all frequencies. Since the database consists of measurements from 25 spatial points around each local point, we compute the *spacial path loss* by averaging the corresponding set of local path losses. Specifically, we perform the linear average

$$PL(d) = 10\log_{10}\left(\frac{1}{25}\sum_{k=1}^{25}10^{\frac{PL^k_{sp}(d)}{10}}\right). \tag{3}$$

From each measured frequency response, we find the local path loss from (2) and the corresponding spacial path loss from (3). For the remainder of this paper, we work with the latter and refer to it simply as path loss.

IV. KEY FINDINGS

We separate our findings into commercial and residential buildings, as well as LOS and NLS paths. For each of the four measured categories, we study the path loss by either pooling data over all buildings or by studying each building separately. Since the center frequency of our measurements is 5GHz, we expect the path loss values taken from the new homes to be comparable with those of our previous measurements [10]. Recall that the previous measurements were taken in 23 homes over a 1.25GHz wide frequency band, centered at 5GHz. The T-R separation of local points ranged from 1 to 15 meters. The path loss values were computed by the same averaging as in (2). Later we will increase the statistical fidelity of our database in residential environments by appending the two large data bases. This

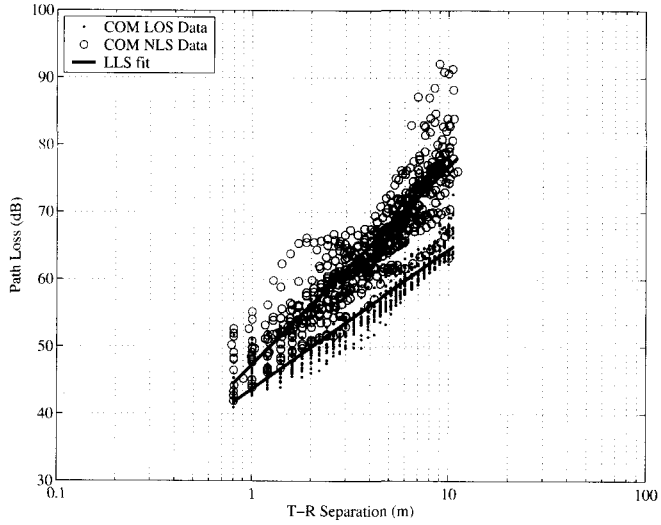

Fig. 3. Path loss vs. T-R separation in residential environments.

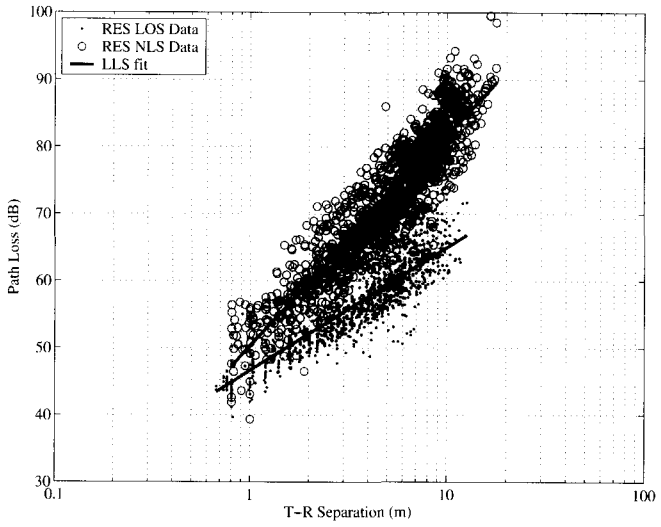

Fig. 4. Path loss vs. T-R separation in commercial environments.

Table 1. The path loss parameters over all buildings.

Environment	PL_0	γ	σ
LOS Commercial	43.7	2.07	2.3
NLS Commercial	47.3	2.95	4.1
LOS Residential	45.9	2.01	3.2
NLS Residential	50.3	3.12	3.8

will result in a combined database of about 2000 path loss points distributed uniformly over distance within 43 homes.

A. *Path Loss Over All Buildings in Each Building*

Initially, we pool path loss values (computed from the new set of measurements only) over all buildings within each of the four categories, and we study their statistics. Using the linear least squares (LLS) method, we fit (1) to the scatter-plots of path loss PL and T-R separation d (with $d_0 = 1$m) and compute PL_0, γ and σ. Table 1 summarizes the parameter values for all new

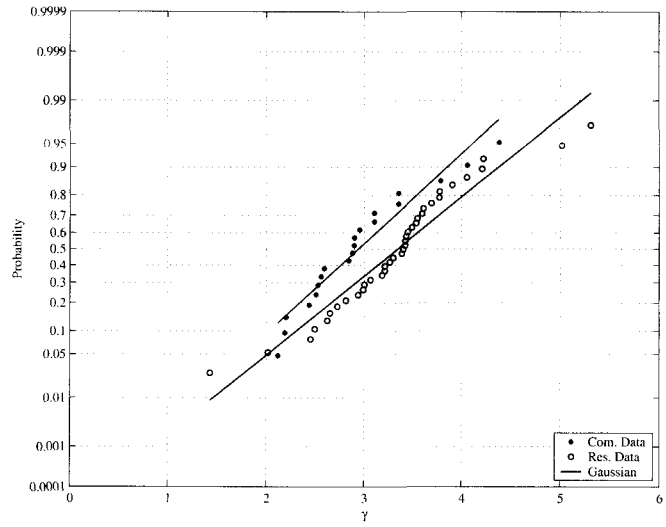

Fig. 5. The distributions of standard deviation of shadowing for commercial and residential buildings on NLS paths.

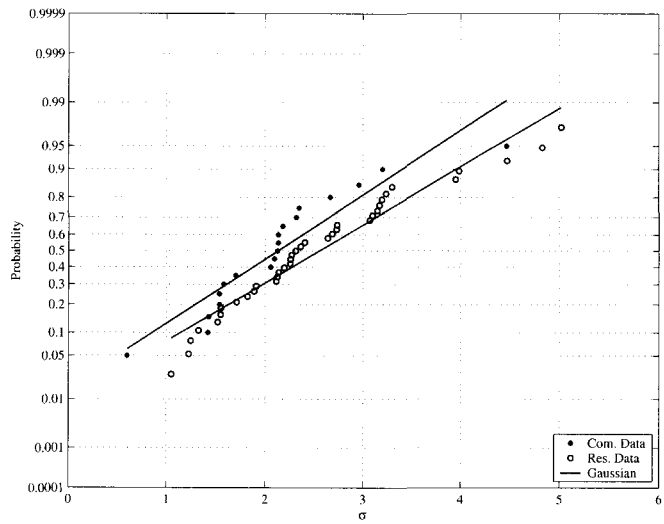

Fig. 6. The distributions of path loss exponent for commercial and residential buildings on NLS paths.

measurements. In comparing the results for homes with those reported in [10] and [11], we find that the path loss parameters are very similar. This justifies our later pooling of the new and previous residential data bases.

Fig. 3 shows scatter plots for LOS and NLS paths in homes (new and previous data pooled), while Fig. 4 shows corresponding scatter plots for commercial buildings (new data only). We see that the main difference between building types is a somewhat higher NLS path loss, on average, in homes. Further measurements in commercial buildings would help test the stability of these results.

B. *Path Loss Parameter Variations Across Buildings*

Differences in building materials, structures and age of buildings cause buildings to exhibit different propagation behaviors. As a result, we expect the slope γ and the standard deviation of shadowing, σ, to vary among buildings. In fact, in [10], we

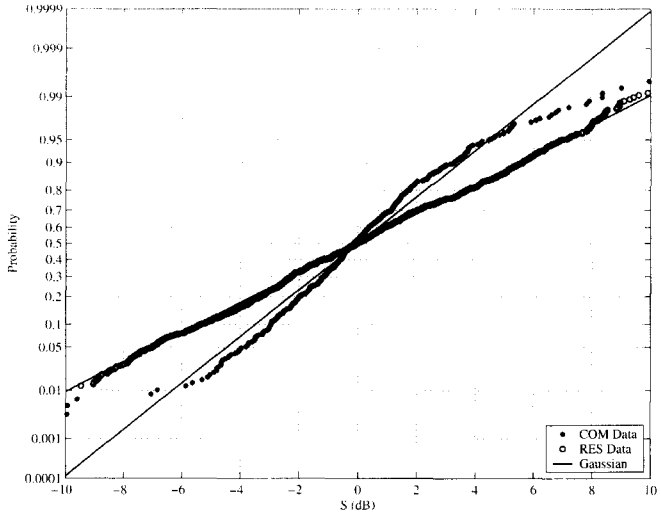

Fig. 7. The shadowing distributions for residential and commercial buildings on NLS paths.

showed how a statistical path loss model can be created by taking γ and σ as random variables over buildings while keeping PL_0 fixed. This follows a similar approach used for path loss modeling in large outdoor cells [13]. We do the same within this work, namely, we fix PL_0 at the mean taken over all buildings and study the statistics over the pool of extracted γ and σ.

Table 2 summarizes the mean and standard deviation of γ and σ for all environments, along with their corresponding values for PL_0. (Here, we denote the mean and standard deviation of γ as μ_γ and σ_γ, respectively, and the mean and standard deviation of σ as μ_σ and σ_σ.) Figs. 5 and 6 show cumulative distribution functions of γ and σ, respectively, in commercial and residential buildings on NLS paths. We observe similar behavior on LOS paths. We find the correlation coefficient between γ and σ in homes to be fairly low (-0.08 and -0.19 for LOS and NLS paths, respectively). Corresponding correlation coefficients for commercial buildings are 0.19 and 0.41 on LOS and NLS paths, respectively.

Finally, we examine the statistics of S, the dB deviation from the median path loss. Fig. 7 shows two CDFs for NLS paths, one for all residences and one for all commercial buildings. Similar results are obtained for LOS paths. For residences in particular, we see excellent agreement with the log-normal assumption for shadow fading.

V. THE PATH LOSS MODEL AND SIMULATIONS

A. The Path Loss Model

We define a statistical path loss model based on (1), with a fixed intercept point PL_0, but treating γ and σ as random variables over buildings. Based on Figs. 5 and 6, we can approximate γ and σ as Gaussian variables.

We could also incorporate the correlation coefficients between them into the model (e.g., using Cholesky factorization [14]). However, our simulation results show little-to-no impact and thus, little justification for including an extra model parameter. Therefore, for simplicity of the model, we assume independence between the parameters γ and σ.

Table 2. Parameter values in path loss model.

Environment	PL_0	μ_γ	σ_γ	μ_σ	σ_σ
LOS Commercial	43.7	2.04	0.30	1.2	0.6
NLS Commercial	47.3	2.94	0.61	2.4	1.3
LOS Residential	47.2	1.82	0.39	1.5	0.6
NLS Residential	50.4	3.34	0.73	2.6	0.9

Table 3. Path loss parameters from simulation.

Environment	PL_0	γ	σ
LOS Commercial	43.7	2.06	2.6
NLS Commercial	46.8	3.03	3.9
LOS Residential	47.2	1.84	3.0
NLS Residential	50.3	3.29	4.4

The Gaussian distribution is completely defined by its first and second moments, allowing us to write

$$\gamma = \mu_\gamma + \sigma_\gamma x_1$$
$$\sigma = \mu_\sigma + \sigma_\sigma x_2,$$

where x_1 and x_2 are iid zero-mean, unit-variance Gaussian random variables which vary from building to building. Then we define the complete statistical path loss model as

$$PL(d) = \underbrace{PL_0 + 10\mu_\gamma \log_{10}(d)}_{\text{Median path loss}} + \underbrace{10\sigma_\gamma x_1 \log_{10}(d) + y\mu_\sigma + yx_2\sigma_\sigma}_{\text{Deviation from median path loss}}. \quad (4)$$

The deviation from the average path loss is a combination of effects from the two zero-mean, unit-variance Gaussian random variables x_1 and x_2 and the zero-mean, unit-variance Gaussian random spatial variable y. We should emphasize that the random variables x_1, x_2, and y should be truncated so as to not take on values outside the range computed from data.

B. Simulations

We simulated the path loss model (4) and compared it to that obtained from measurements. For each environment category, we generated 20 realizations of x_1 and x_2, representing the number of simulated buildings. We also generated 98 pairs of d and y for each pair of x_1 and x_2, representing the distance and shadowing at 98 locations within each building simulated.

In Figs. 8 and 9, we show the comparison between the simulated results and measured scatter plots of NLS path loss in residential and commercial buildings, respectively. We observed similar results for LOS paths. Parameters from the simulations are summarized in Table 3 and can be compared with those in Table 1. The discrepancies are minor. Moreover, recall that the residential data used to obtain Table 1 were from new measurements only, while the data used to obtain Table 3 included this database together with the one reported in [10]. This, we find, is the cause of most of the differences between these tables. We

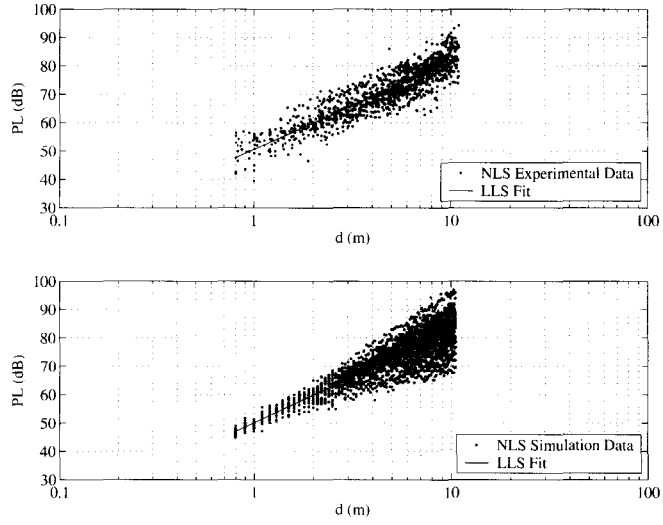

Fig. 8. Path loss: Simulated vs. measured in residential buildings.

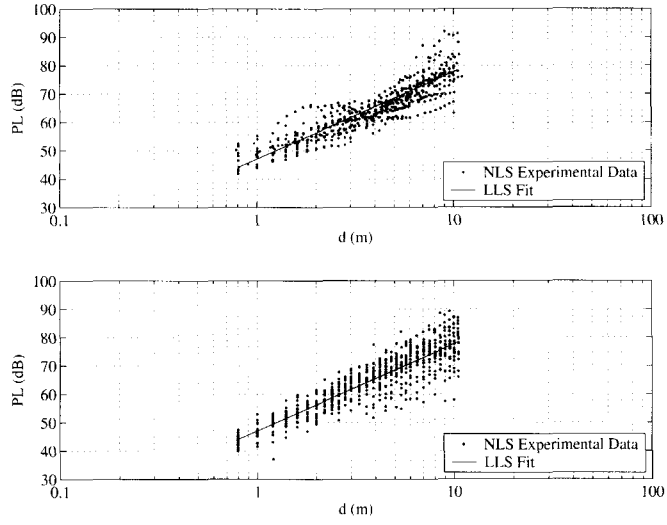

Fig. 9. Path loss: Simulated vs. measured in commercial buildings.

conclude that our model succeeds in generating path loss statistics very close to those of the database.

VI. CONCLUSIONS

We have reported path loss findings from extensive measurements of a wireless UWB channel in 20 commercial buildings and 43 homes. We used a previously proposed statistical path loss model as a basis for modeling the path loss of the channel and confirmed its goodness. Moreover, the agreement of the current model for residences with those reported in [10] and [11] is excellent. The earlier model was based on measurements over 1.25GHz, without spatial averaging, and for a different population of homes (or some of the same homes but different paths). The repeatability of the model, combined with its relative simplicity, makes it both reliable and useful for characterizing indoor path loss. Further measurements in commercial buildings would help to establish model stability for that category.

VII. ACKNOWLEDGEMENT

The authors thank Alexander Hiamovich and Haim Grebel for use of their anechoic chamber at the New Jersey Institute of Technology; Chris Rice of AT&T Labs-Research, for valuable comments and suggestions on the hardware set-up; and lastly but not least, all the homeowners from AT&T Labs and Harvard University who graciously allowed us to invade their premises with our measurements.

REFERENCES

[1] FCC Document 00-163: Revision of Part 15 of the Commission's Rules Regarding Ultra-Wideband Transmission Systems, ET Docket No. 98-153, April 22, 2002.

[2] IEEE 802.15.3, IEEE standard for wireless personal networks (WPAN), URL: http://www.iece802.org/15/pub/TG3a.html.

[3] A. A. Saleh and R. A. Valenzuela, "A statistical model for indoor multipath propagation," *IEEE J. Select. Areas Commun.* vol. 5, pp. 128–137, Feb. 1987.

[4] S. J. Howard and K. Pahlavan, "Measurement and analysis of the indoor radio channel in the frequency domain," *IEEE Trans. Instrum. Measure.*, vol 39, pp. 751–755, Oct. 1990.

[5] T. S. Rappaport, S. Y. Seidel, and K. Takamizawa, "Statistical channel impulse response models for factory and open plan building radio communication system design," *IEEE Trans. Commun.*, vol. 39, pp. 794–806, May 1991.

[6] H. Hashemi, "The indoor propagation channel," *Proc. IEEE*, vol. 81, pp. 943–968, July 1993.

[7] D. Cassioli, M. Z. Win, and A. Molisch, "The ultra-wide bandwith indoor channel: From statistical model to simulations," *IEEE J. Select. Areas Commun.*, vol. 20, pp. 1247–1257, Aug. 2002.

[8] J. Foerster, "Channel modeling sub-committee report final," IEEE P802.15-02/368r5-SG3a.

[9] R. Addler *et al.*, "UWB channel measurements for the home environment," *UWB Intel Forum*, Oregon, 2001.

[10] S. S. Ghassemzadeh *et al.*, "A statistical path loss model for in-home UWB channels," in *Proc. IEEE Conf. Ultra Wideband Systems and Technologies*, pp. 59-64, May 2002.

[11] S. S. Ghassemzadeh *et al.*, "Measurement and modeling of an ultra-wideband indoor channel," *IEEE Trans. Commun.*, Dec. 2003.

[12] S. S. Ghassemzadeh *et al.*, "UWB indoor delay profile model for residential and commercial buildings," in *Proc. IEEE VTC-Fall*, 2003.

[13] V. Erceg *et al.*, "An empirically based path loss model for wireless channels in suburban environments," *IEEE J. Select. Areas Commun.*, vol. 17, pp. 1205–1211, July 1999.

[14] C. D. Meyer. *Matrix analysis and applied linear algebra*, SIAM, 2000.

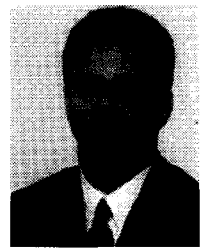

Saeed S. Ghassemzadeh received his B.S., M.S., and Ph.D. degree in Electrical Engineering from the City University of New York in 1989, 1991, and 1994, respectively. From 1989 to 1995, he was with InterDigital Communications. Corp. working as a principal research scientist on propagation channel modeling and spread spectrum access techniques. He then joined AT&T Bell-Labs in 1995 where he was involved in development of CDMA based technology wireless systems and conducted research in satellite access techniques, coding, fixed/mobile access technologies, and many wireless propagation channel measurement/modeling. Currently, he is a principal technical staff member in broadband networking technology research department at AT&T Labs-Research, Florham Park, NJ. His current research includes providing techniques for performance enhancement of free space optical systems, wireless channel propagation measurement/modeling, wireless system architecture and design for improving capacity/performance/range of wireless local area networks, and wireless personal area networks devices. He is a senior member of IEEE and IEEE communication society.

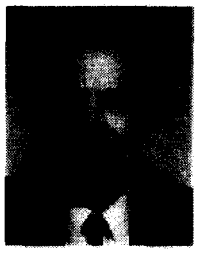

Larry J. Greenstein received the B.S., M.S., and Ph.D degrees in electrical engineering from Illinois Institute of Technology, Chicago, IL, in 1958, 1961, and 1967, respectively. From 1958 to 1970, he was with IIT Research Institute, Chicago, IL, working on radio frequency interference and anti-clutter airborne radar. He joined Bell Laboratories, Holmdel, NJ, in 1970. Over a 32-year AT&T career, he conducted research in digital satellites, point-to-point digital radio, lightwave transmission techniques, and wireless communications. For 21 years during that period (1979-2000), he led a research department renowned for its contributions in these fields. His research interests in wireless communications have included measurement-based channel modeling, microcell system design and analysis, diversity and equalization techniques, and system performance analysis and optimization. He is now a Research Professor at Rutgers WINLAB, Piscataway, NJ, working in the areas of ultra-wideband (UWB) techniques, wireless LANs, sensor networks, and channel modeling. He is an AT&T Fellow and an IEEE Life Fellow, has won two best paper awards, and has been a Guest Editor, Senior Editor and Editorial Board Member for numerous publications.

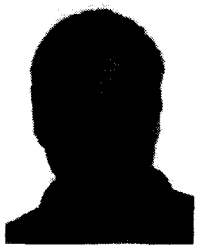

Aleksandar Kavčić was born in Belgrade, Yugoslavia. He received the Dipl. Ing. degree in Electrical Engineering from Ruhr-University, Bochum, Germany in 1993, and the Ph.D. degree in Electrical and Computer Engineering from Carnegie Mellon University, Pittsburgh, Pennsylvania in 1998. Since 1998, he has been with the Division of Engineering and Applied Sciences at Harvard University where he is currently the John L. Loeb Associate Professor of the Natural Sciences. From 1998 until 2002, he was an Assistant Professor of Electrical Engineering at Harvard University. He held short-term research positions at Seagate Technology in 1995, Read-Rite Corporation in 1996, and Quantum Corporation from 1997 to 2000. His research spans topics in Communications, Signal Processing, Information Theory and Magnetic Recording. He received the IBM Partnership Award in 1999 and the NSF CAREER Award in 2000. He is presently serving on the editorial board of the IEEE Transactions on Information Theory as Associate Editor for Detection and Estimation

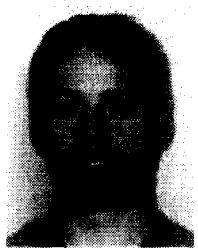

Thorvardur Sveinsson received his B.Sc. degree in Electrical Engineering from the University of Iceland in 2000. In 2003 he graduated from Harvard University, with a M.E. degree in Electrical Engineering. From 2000- 2001 he worked as a Software Engineer at the Icelandic Investment Bank. He is presently working as an Engineer at Kogun Air Defense System, Reykjavik Iceland.

Vahid Tarokh received his Ph.D. degree in Electrical Engineering from the University of Waterloo, Ontario, Canada. He is currently a professor of electrical engineering' at the Division of Engineering and Applied Sciences of Harvard University. He has received a number of awards including the 1987 Gold Tablet of The Iranian Math Society, the 1995 Governor General of Canada's Academic Gold Medal, the 1999 IEEE Information Theory Society Prize Paper Award, and the 2001 Alan T. Waterman Award. In 2002, he was selected as one of the top 100 young inventors of the year by the Technology Review Magazine. His honorary degrees include those from Harvard and Windsor. He is a senior member of IEEE and IEEE communication society.